

Chemopreventive Effects of Pterostilbene on Urethane-Induced Lung Carcinogenesis in Mice via the Inhibition of EGFR-Mediated Pathways and the Induction of Apoptosis and Autophagy

Rong-Jane Chen,^{†,‡,||} Shang-Jie Tsai,[†] Chi-Tang Ho,[§] Min-Hsiung Pan,[⊗] Yuan-Soon Ho,^{#,⊥,||} Chih-Hsiung Wu,^{*,⊥,Δ} and Ying-Jan Wang^{*,†}

[†]Department of Environmental and Occupational Health, National Cheng Kung University Medical College, Tainan, Taiwan

[‡]Graduate Institute of Clinical Medicine, Taipei Medical University, Taipei, Taiwan

[§]Department of Food Science, Rutgers University, New Brunswick, New Jersey, United States

[⊗]Department of Seafood Science, National Kaohsiung Marine University, Kaohsiung, Taiwan

[#]School of Medical Technology and Biotechnology, Taipei Medical University, Taipei, Taiwan

[⊥]Center of Excellence for Cancer Research, Taipei Medical University, Taipei, Taiwan

^ΔDepartment of Surgery, School of Medicine, Taipei Medical University–Shuang Ho Hospital, Taipei, Taiwan

ABSTRACT: Lung cancer is the most commonly diagnosed cancer and the leading cause of cancer deaths globally. Due to the lack of successful chemopreventive agents for lung cancer, there is an emerging need to evaluate new and effective agents for lung cancer prevention. Pterostilbene, a naturally occurring analogue of resveratrol, has been reported to be an effective chemopreventive agent against many cancers. The aim of this study is to investigate the chemopreventive effects of pterostilbene in urethane-induced murine lung tumors. Pretreatment with pterostilbene at 50 or 250 mg/kg significantly reduced tumor multiplicity by 26 and 49%, respectively. Pterostilbene also significantly inhibited tumor volume by 25 and 34% and decreased the tumor burden per mouse by 45 and 63%, respectively. The mechanisms by which pterostilbene suppresses lung tumorigenesis have been investigated in lung tissues and homogenates. The results indicate that the pterostilbene-mediated chemopreventive effects in vivo were a result of the inhibition of epidermal growth factor receptor (EGFR) and its downstream pathways, leading to retarded cell cycle progression, and of the induction of apoptosis and autophagy during urethane-induced lung tumorigenesis.

KEYWORDS: chemopreventive, pterostilbene, urethane, EGFR, autophagy

■ INTRODUCTION

Lung cancer is the most commonly diagnosed cancer, the leading cause of cancer death in males, and the second leading cause of cancer death in females globally.¹ Because of the lack of success in treating advanced lung cancer, there is an increasing emphasis on preventing lung cancer through smoking cessation. Smoking cessation is clearly the most effective intervention to reduce lung cancer incidence; however, smoking rates have continued to increase worldwide, and ex-smokers still carry a significant risk for lung cancer. Moreover, lung cancers are also reported associated with other factors such as environmental influences or nutrition.² Hence, the incidence of lung cancer decreases only slowly after smoking cessation, and the lung cancer epidemic will continue for many years due to increased smoking rates and environmental carcinogen exposure.³ Therefore, additional preventive approaches are needed to reduce the risk of lung cancer. Chemopreventive agents, which could reverse, suppress, prevent, or delay the carcinogenic process by blocking the development of early lesions or by inhibiting the progression to an invasive cancer, offer one such alternative. Chemoprevention has been applied with some early success in high-risk groups for breast, prostate, colon, and skin cancers, but not for lung cancer.³ There remains a need to identify effective agents with

acceptable safety and efficacy profiles for lung cancer prevention.

Pterostilbene (*trans*-3,5-dimethoxy-4'-hydroxystilbene) is a naturally occurring phytoalexin identified in several plants in the genus *Pterocarpus*, in *Vitis vinifera* leaves, in some berries (e.g., blueberries and cranberries), and in grapes.⁴ Pterostilbene, an analogue of the well-studied resveratrol, has pharmacological properties similar to those of resveratrol, but has several advantages compared to resveratrol, including more lipophilicity, which increases oral absorption and the potential for higher cellular uptake, as well as a longer half-life than resveratrol.⁵ Indeed, pterostilbene is reported to be more potent than resveratrol in preventing azoxymethane (AOM)-induced colon tumorigenesis.⁶ Pterostilbene also has diverse pharmacological activities including antioxidant, anti-inflammatory, cancer prevention activity, and anticancer effects in a number of cancer cell lines, including breast, melanoma, colon, liver, gastric, and bladder.^{4,7–9} The study of the molecular mechanisms of pterostilbene action revealed that pterostilbene

Received: June 28, 2012

Revised: October 30, 2012

Accepted: October 31, 2012

Published: October 31, 2012

can suppress colon tumorigenesis and cell proliferation in animal models through reduced gene expression of Myc, cyclin D, nuclear factor- κ B (NF κ B) p65, inducible NO synthase (iNOS), cyclooxygenase-2 (COX-2),^{10,11} vascular endothelial growth factor (VEGF), matrix metalloproteinases (MMPs), and PI3K/Akt. Pterostilbene also induces apoptosis and the NF-E2 related factor 2 (Nrf2)-mediated antioxidant signaling pathways.^{6,12} These beneficial effects of pterostilbene make it a potential chemopreventive agent for many cancers. However, its chemopreventive effects and the underlying mechanisms in lung tumorigenesis remain unclear.

Lung tumorigenesis results from a series of genetic and epigenetic alterations in pulmonary epithelial cells (including *K-Ras* mutations, *p53* mutations, and epidermal growth factor receptor (EGFR) overexpression).¹³ EGFR is a membrane-bound tyrosine kinase that forms protein homo- or heterodimers upon ligand binding, leading to the activation of the four major signaling pathways: (1) the Ras/MAPK pathway, which promotes cell proliferation by driving cell cycle progression from the G1 to the S phase; (2) the PI3K/Akt pathway, which activates antiapoptotic and prosurvival signals; (3) the Stat3 signaling pathway, which induces cell invasion and metastasis;^{14,15} and (4) the NF κ B pathway, which is a key regulator in the production of pro-inflammatory cytokines, cell cycle proteins, antiapoptotic proteins, and growth factors.¹⁶ These signaling pathways are now recognized as important mediators of lung carcinogenesis.¹⁶ EGFR signaling may be up-regulated by EGFR gene mutation, increased gene copy number, and EGFR protein overexpression. EGFR overexpression and mutations have likewise been observed in premalignant lung epithelium, squamous cell carcinoma, metastatic nonsmall cell lung carcinoma, suggesting that EGFR overexpression and mutations could be involved in lung tumorigenesis.^{14,17} These studies indicated that the inhibition of key signaling mediators downstream of EGFR can lead to clinical effects in the prevention and treatment of lung cancer with robust EGFR activity. In our current study, we focused on the regulation of EGFR signaling and its downstream pathways by pterostilbene.

Chemically induced murine adenocarcinoma models contain many of the same histology, gene expression, and genetic alterations found in human lung tumors (including *p16*, *Rb*, *APC*, and *p53* or the mutation of oncogenes such as *K-Ras*), and these are good models for the evaluation of chemopreventive agents.¹⁸ Through modulation of *K-Ras*, *p53*, and related signaling pathways, chemopreventive agents can induce apoptosis and autophagy that limit malignant transformation and inhibit tumor progression.¹⁹ Therefore, targeting to those signaling pathway-triggered activations of apoptosis and autophagy could be beneficial in the prevention of lung cancer. Herein, we investigate the chemopreventive efficacy of pterostilbene on urethane-induced lung tumorigenesis in A/J mice. Lung cancer development could be derived by EGFR leading to Ras/MAPK, EGFR/PI3K/Akt, and Stat3 activation, and pterostilbene should exert its chemopreventive effects through modulating, at least in part, EGFR and its downstream cellular signaling pathways, leading to cell cycle arrest, apoptosis, and autophagy. Our current findings support this hypothesis, suggesting that pterostilbene warrants further development as a chemopreventive agent for lung cancer.

MATERIALS AND METHODS

Chemicals and Reagents. Pterostilbene (96% purity) was a gift from Sabinsa Corp. (East Winsor, NJ, USA). Urethane and corn oil were from Sigma (St. Louis, MO, USA). Primary antibodies against cyclin D1, cyclin A, PCNA, p21, p27, p53, EGFR, Akt, phospho-Akt, mTOR, phospho-mTOR, ERK1/2, phospho-ERK1/2, Stat3, phospho-Stat3 Ser727, p65, phospho-p65, phospho-IKK, IKK, I κ B α , β -actin, GAPDH, and horseradish peroxidase (HRP)-conjugated anti-mouse and anti-rabbit secondary antibodies were purchased from Cell Signaling (Beverly, MA, USA). The anti-LC3 antibody was obtained from MBL (Woburn, MA, USA), and the cleaved caspase-3 antibody was purchased from Epitomics, Inc. (Burlingame, CA, USA).

Mouse Models of Lung Carcinogenesis. Five-week-old male A/J mice, acquired from the Laboratory Animal Center of the National Cheng Kung University Medical College, were housed five mice per cage in a pathogen-free environment, maintained on Lab Diet 5010 (PMI Feed, Inc., USA) at 24 ± 2 °C and $50\% \pm 10\%$ relative humidity, and subjected to a 12 h light/12 h dark cycle. Upon arrival, the mice were randomized into different groups as follows: (1) corn oil (control), (2) 1 mg/g urethane (positive control), (3) urethane + low-dose pterostilbene (50 mg/kg), and (4) urethane + high-dose pterostilbene (250 mg/kg). Each group contained 15 mice. To induce tumors, mice received a single intraperitoneal (ip) injection of urethane (1 mg/g) in saline. The experimental design is shown in Figure 1. Animal studies were approved by the Laboratory Animal

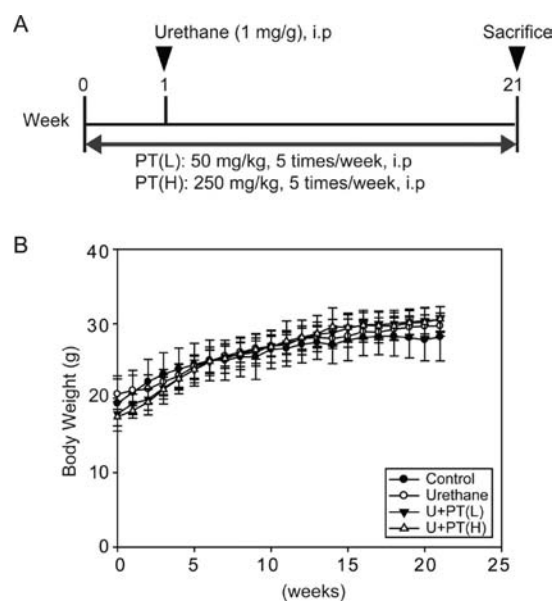


Figure 1. Experimental design to assess the inhibition of urethane-induced lung carcinogenesis in A/J mice by pterostilbene (PT). (A) This study was designed to allow for 1 week of pretreatment with PT, followed by urethane at 1 mg/g. PT doses were given for an additional 20 weeks after treatment with urethane. At the end of the study, mice were euthanized and the lungs were harvested. (B) Weight curves of mice in various treatment groups. All treatment groups had similar weight gain throughout the experiment. U, urethane; PT(L), pterostilbene low dose, 50 mg/kg; PT(H), pterostilbene high dose, 250 mg/kg.

Center of the National Cheng Kung University Medical College and performed according to the local guidelines for animal care and protection.

Treatment with Pterostilbene (PT) and Evaluation of Tumor Growth. Pterostilbene was dissolved in corn oil to make working solutions. A/J mice were given ip injections of pterostilbene at a low dose (50 mg/kg) or a high dose (250 mg/kg) for 1 week prior to initiation of urethane exposure and 5 times per week continuing until the termination of the experiment (up to 20 weeks after urethane

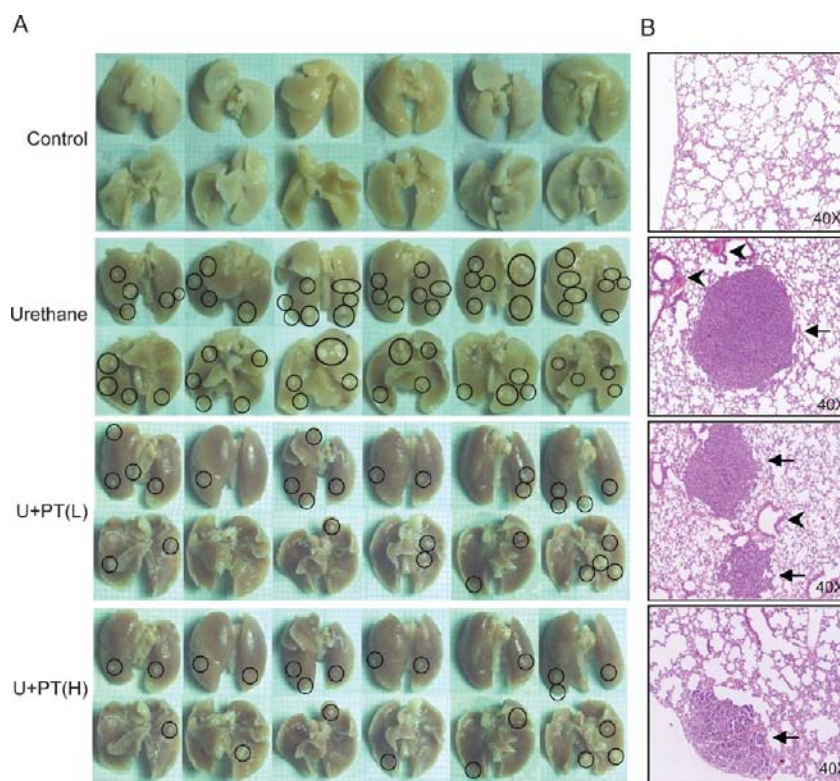


Figure 2. Tumor pathology of lungs in urethane- and PT-treated mice. (A) Images of the lung surface indicate that urethane-treated mouse lungs presented with numerous visible lesions (black circles). (B) Histological characteristics of mouse lungs stained with H&E from control, urethane, PT(L), and PT(H) treatment groups. Arrows indicate the adenocarcinoma in the lungs of mice. Invasive tumors are labeled by arrowheads. U, urethane; PT(L), pterostilbene low dose, 50 mg/kg; PT(H), pterostilbene high dose, 250 mg/kg.

exposure). The experiment was terminated after the 20th week of urethane injection, with serial body weights taken weekly during the course of the experiment.

Histopathological Analysis. At the end of the experiments, all mice ($n = 15$ in each group) were euthanized under ether anesthesia, and the lungs were removed and examined for the presence of gross tumors at necropsy. The whole lungs removed from three mice of each group were kept at -80°C for Western blotting analysis. The lungs removed from the remaining 12 mice of each group were preserved in 10% buffered formalin. These formalin-fixed whole lungs were used for calculating lung nodules and then provided for histology examination and immunohistochemistry. Tumor nodules on the lung surfaces were then counted as an index of multiplicity. The tumor diameter was measured with the aid of digital calipers under a microscope. Maximal diameters of each lesion were determined for each anatomical direction (transaxial, coronal, and sagittal), and the mean diameter was determined. Tumor volume was determined by measuring the diameter of each tumor. The radius ($r = \text{diameter}/2$) was determined, and the total tumor volume was calculated by using the equation $\text{volume} = (4/3)\pi r^3$.²⁰ Lung tumor development was estimated quantitatively by measuring the number, volume, and tumor load (sum of volume per lung). Differences in the tumor sizes (volume) of PT-treated and urethane-treated groups were compared using the chi-square (χ^2) test.

Histology and Immunohistochemistry. For histological examination, serial tissue sections ($4\ \mu\text{m}$) were sliced from paraffin-embedded, formalin-fixed lungs and stained with hematoxylin and eosin (H&E). For immunohistochemistry, tissue sections were deparaffinized and hydrated. Antigen retrieval was performed in a microwave for 20 min with citrate buffer (pH 6.0), and then the slides were immersed in 3% H_2O_2 for 20 min to block the activity of endogenous peroxidase. After blocking, the slides were incubated overnight at 4°C using antibodies for PCNA, caspase-3, and LC3 at a 1:100 dilution and then incubated with the appropriate secondary antibody for 1 h at room temperature. The slides were developed with

the STARRTREK Universal HRP detection kit (Biocare Medical, Concord, CA, USA) according to the manufacturer's protocol, and the slides were counterstained with hematoxylin. The labeling index was expressed as the average number of immunostained cells per field divided by the total number of lung epithelial cells and multiplied by 100 in three randomly selected 400X magnified fields per slide. All IHC analyses were performed in three slides from different mice.

Western Blot Analyses. Randomized frozen lung samples from three individual mice from control, urethane-treated, and pterostilbene-treated groups were homogenized, and lysates were subjected to gel electrophoresis and immunoblotting. Immunoreactive proteins were visualized with a chemiluminescent detection system (PerkinElmer Life Science, Inc., Boston, MA, USA) and BioMax LightFilm (Eastman Kodak Co., New Haven, CT, USA) according to the manufacturer's instructions.

Statistical Analyses. Results are expressed as the mean \pm standard error of the mean (SEM). Experimental data were analyzed using Student's t test. Differences were considered to be statistically significant when the p value was <0.05 .

RESULTS

Effects of Pterostilbene on the Incidence and Multiplicity of Lung Lesions. Lung adenomas were induced in A/J mice by ip injection of urethane at approximately 7 weeks of age. To test the potency of PT in preventing lung cancer development, we applied two doses of PT (low dose, PT(L), 50 mg/kg; high dose, PT(H), 250 mg/kg) to the urethane-induced lung carcinogenesis model. PT was initiated 1 week before urethane injections and continued for an additional 20 weeks (Figure 1). There were no signs of toxicity when mice were observed once a week for signs of toxicity, such as fur color, motor and behavioral abnormalities, and palpable masses. Mice in the different treatment groups had similar body weights

at the beginning of the experiment, and the body weights remained no different among all groups during the experiments (Figure 1B). These results indicated that treatment with PT did not induce any remarkable toxicity in mice.

At necropsy after 20 weeks of urethane treatment, the numbers of tumors on the surface of the lungs were counted (Figure 2A). A significant decrease in the number and size of tumors was observed not only on the surface of lungs but also in the lung sections (Figure 2B). Histopathological examination indicated a malignant and invasive phenotype with urethane-induced carcinoma cells that can be seen infiltrating to the adjacent alveoli and invading the bronchus (Figure 2B). Most notably, the severity of histopathology was significantly reduced in mice treated with high-dose PT, when compared to the urethane-treated groups, with tumors classified as noninvasive (Figure 2B).

Pterostilbene Reduced the Multiplicity of Urethane-Induced Pulmonary Surface Tumors. Our results showed that all mice treated with urethane develop tumors. As shown in Table 1, mice that received 1 mg/g urethane bear an average of

Table 1. Effects of Pterostilbene on Urethane-Induced Lung Tumor Development (Multiplicity, Volume, and Burden) in A/J Mice^a

	urethane	PT(L), 50 mg/kg	PT(H), 250 mg/kg
no. of mice	12	12	12
no. of lung tumors	409	302	210
no. of tumors per mouse	34.1 ± 6.09	25.2 ± 6.6*	17.5 ± 4.9*,†
reduction in tumor multiplicity (%)		26	49
average tumor volume per mouse	1.01 ± 0.31	0.75 ± 0.19*	0.66 ± 0.16*
inhibition of tumor volume (%)		25	34
tumor burden per mouse	33.9 ± 8.58	18.69 ± 6.00*	12.6 ± 4.62*,†
inhibition of tumor burden (%)		45	63

^aPT(L), pterostilbene low dose, 50 mg/kg; PT(H), pterostilbene high dose, 250 mg/kg. The results are presented as the mean ± SEM. *, $p < 0.05$, significantly lower than urethane-treated group; †, $p < 0.05$ significantly lower than PT(L)-treatment group.

34.1 ± 6.9 tumors per mouse. Urethane-treated mice given 50 mg/kg PT showed 25.2 ± 6.6 tumors per mouse, corresponding to a 26% reduction in multiplicity. A higher dose of PT (250 mg/kg) significantly reduced lung tumor numbers to 17.5 ± 4.9, a reduction in multiplicity by 49% (Table 1). In addition, PT significantly inhibited tumor volume by 25 and 34% in PT 50 and 250 mg/kg treated groups, respectively (Table 1). The large sizes and more histologically advanced tumors in urethane-treated mice are shown in Figure 2B. PT also decreased the tumor burden per mouse by 45 and 63% in 50 and 250 mg/kg PT treatment groups, respectively (Table 1). These results indicated that PT retarded lung cancer development by limiting tumor multiplicity, tumor volume, and tumor burden, suggesting that PT could be a potential inhibitor for the development of lung adenoma.

Pterostilbene Decreased the Sizes of Tumors of Urethane-Induced Pulmonary Surface Tumors.

Pterostilbene also decreased the sizes of tumors. Upon counting the lung tumors, the diameter of the tumors was categorized into three classes: >1.5, 1–1.5, and <1 mm (Figure 3). Most of the

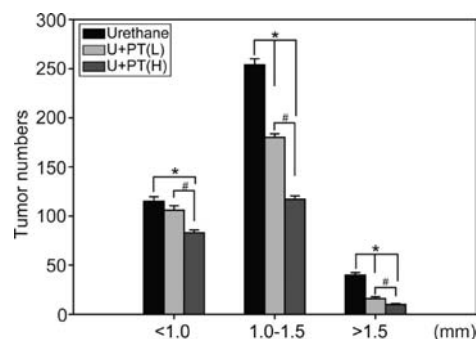


Figure 3. Effect of PT on the size of lung tumors. Mice were sacrificed 20 weeks after exposure to urethane. The tumor diameter was divided into three categories: <1, 1–1.5, and >1.5 mm. U, urethane; PT(L), pterostilbene low dose, 50 mg/kg; PT(H), pterostilbene high dose, 250 mg/kg. *, $p < 0.05$, significantly lower than urethane-treated group in different diameter category; #, $p < 0.05$ significantly lower than PT(L) treatment group in different diameter category. Mean ± SEM; $n = 12$.

tumors, regardless of treatment, had a diameter of 1–1.5 mm. In the urethane groups, multiplicities of lung tumors with a diameter of <1, 1–1.5, and >1.5 mm were 115 ± 4.6, 254 ± 6.1, and 40 ± 2.4 tumors per mouse, respectively. The high dose of PT(H) significantly decreased the incidence of all size categories of lung tumors with a diameter >1.5, 1–1.5, and <1 mm to 83 ± 2.8, 117 ± 3.5, and 10 ± 0.8 tumors per mouse, respectively. The results indicated that the frequency of all tumor sizes was reduced by the high dose of pterostilbene. Meanwhile, in mice given the lower dose of PT (50 mg/kg), the multiplicity with a diameter of 1–1.5 and <1 mm was significantly reduced (180 ± 3.6 and 16 ± 1.9 tumors per mouse, respectively).

Molecular Mechanisms of Pterostilbene in Lung Cancer Chemoprevention.

When considering the mechanisms of PT-mediated changes in tumor multiplicity, we proposed the hypothesis that PT inhibits EGFR expression, leading to the attenuation of lung tumorigenesis. Figure 4A shows a Western blot analysis of lung homogenates of control, urethane-treated, and PT-treated animals, in which the treatment of PT blocked urethane-induced EGFR overexpression by 2-fold compared with control (Figure 4A). To further confirm the pivotal role of EGFR in lung tumorigenesis, we also analyzed its downstream signaling, including Akt/mTOR and ERK1/2 pathways. These pathways were suggested to play a central role in tumorigenesis by regulating the expression of metabolic, prosurvival, antiapoptosis, inhibition of autophagic, and invasion-related pathways.²⁰ Compared with the level in mice treated with urethane alone, PT treatment led to a significant decrease in phosphorylation of Akt/mTOR and ERK1/2 proteins parallel to control (Figure 4A).

On the basis of the reported intracellular signaling pathways activated by the EGFR, we proposed that transcriptional factors such as NFκB and Stat3, which are downstream of EGFR, could contribute to lung tumorigenesis.¹⁵ Stat3 and NFκB not only enhance inflammation but also enhance carcinogenesis. We

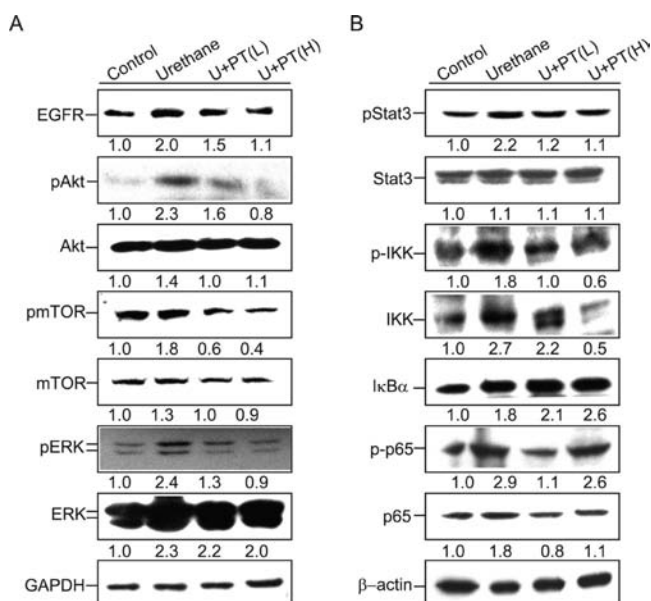


Figure 4. Western blot analysis of the effects of PT on the inhibition of EGFR and its downstream signaling pathways. (A) Lung homogenates were collected from control and urethane-, PT(L)-, and PT(H)-treated mice. Expression of EGFR, p-Akt, Akt, p-mTOR, mTOR, p-ERK, and ERK and (B) p-Stat3, Stat3, p-IKK, IKK, IκBα, p-p65, and p65 was detected by Western blotting analysis. PT(L), pterostilbene low dose, 50 mg/kg; PT(H), pterostilbene high dose, 250 mg/kg. Equal protein loading was determined by anti-GAPDH (A) or anti-β-actin antibodies. Each sample was run on separate Western blot, and the results of three independent experiments by using three individual mouse lungs were averaged. Representative data from one of three independent experiments are shown. The number below each line indicates the relative intensity of protein expression compared to the control group (defined as 1).

analyzed lung homogenates from all treatment groups for p-Stat3, Stat3, p-IKK, IKK, IκBα, p-p65, and p65. We found that PT treatment significantly decreased by nearly half p-Stat3 expression when compared to the urethane-treated groups (Figure 4B). Similarly, both doses of PT diminished the degradation of IκBα, which was supported by diminishing the activation of IKK (Figure 4B). The expressions of p-p65 and p65 were also decreased in the PT(L) group (1.1-fold compared to control), but increased in the PT(H) group (2.6-fold compared to control). This could be due to unequal protein loading as determined by β-actin loading control (Figure 4B). Besides, it is interesting that the expression of IκBα increased by 1.8-fold in the urethane treatment group compared to control groups (Figure 4B). According to previous studies, IκBα is strongly induced by NFκB to control NFκB activity in a negative feedback loop,²¹ so IκBα overexpression in urethane-treated groups could be due to activation of NFκB. However, the new expressed IκBα in urethane-treated group must escape proteasome degradation prior to entering the nucleus and binding to NFκB. Nevertheless, the increased IκBα may still not be sufficient to inhibit NFκB activity because rapid protein degradation could occur. Taken together, these results suggest that reduction of EGFR expression parallels the antineoplastic activity of PT, and these effects could be related to the down-regulation of Akt/mTOR, ERK1/2, Stat3, and NFκB signaling pathways.

Chemopreventive Effects of Pterostilbene Could Be through Reduced Cell Proliferation and the Induction of

Apoptosis and Autophagy. Because we observed PT-mediated decreases in the number and size of lung tumors, we next examined the effects of chronic PT treatment on cell proliferation in lung tissues and lung homogenates after 20 weeks of urethane treatment. Of note, both doses of PT decreased urethane-induced PCNA expression in lung tissues compared to urethane-treated groups (Figure 5A). Suppressed PCNA expression was further confirmed by Western blot analysis, as shown in Figure 5B. Akt and Stat3 are known to regulate cell cycle progression; thus, we further determined the effects of PT on cell cycle-regulated proteins in lung homogenates. The results demonstrated that PT suppressed proteins important for cell cycle progression, such as cyclin D1 and cyclin A (Figure 5C). In addition, PT enhanced the expression of tumor suppressor p53 and CDK inhibitors p27 and p21 (Figure 5C). The results clearly indicated that PT suppressed cell proliferation and restored the expression of tumor suppressors in response to urethane.

In addition, the inhibition of EGFR and its related downstream signaling by PT may also lead to apoptosis and autophagy, which are important mechanisms for chemoprevention.¹⁹ The expression of proteins related to apoptosis and autophagy were analyzed by immunohistochemistry and Western blot. As shown in Figure 5A,B, mice treated with PT exhibited expression levels of cleaved caspase-3 and LC3-II that were increased compared to the urethane-treated group. In summary, these findings suggest that the PT-mediated chemopreventive effects *in vivo* may in part be correlated with the inhibition of EGFR-related pathways, leading to retarded cell cycle progression and the induction of apoptosis and autophagy during urethane-induced lung tumorigenesis.

DISCUSSION

Due to a lack of successful chemopreventive agents for lung cancer, there is a widely recognized need to evaluate new and effective agents for lung cancer prevention. The concept of cancer chemoprevention has gained increasing attention because it is cost-effective and avoids the side effects of cancer treatment.²² Before chemopreventive agents are moved to clinical trials, it is important to perform a comprehensive evaluation using evidence from epidemiology, cell biology, and preclinical studies. Accordingly, the EGFR and its downstream signaling pathways have been strongly implicated in the development of lung cancer. The development of inhibitors of EGFR, COX-2, and Ras had been suggested as useful strategies in cancer chemoprevention. However, safety is the major concern with these pharmaceutical agents. Natural compounds have been presumed to be safer than synthetic compounds due to their presence in the diet and wide availability.²² Pharmacokinetics plays a pivotal role in drug discovery and development. On the basis of chemical structure, pterostilbene has a dimethyl ether structure that enhanced its lipophilicity and increased its membrane permeability. However, the pharmacokinetic results of PT are sparse, and the absolute bioavailability of PT remained unknown. There is only one report of the study of the absolute bioavailability of PT by intravenous or oral administration in SD rats. The results indicated that after oral administration of pterostilbene (10 mg/kg), the plasma pterostilbene increased gradually but the maximum concentration (C_{max}) was quite low (141 ± 71 ng/mL), and the bioavailability (F%) of PT by oral administration reached only $12.5 \pm 4.7\%$.²³ In addition, an unidentified metabolite was present in all plasma samples. Our previous

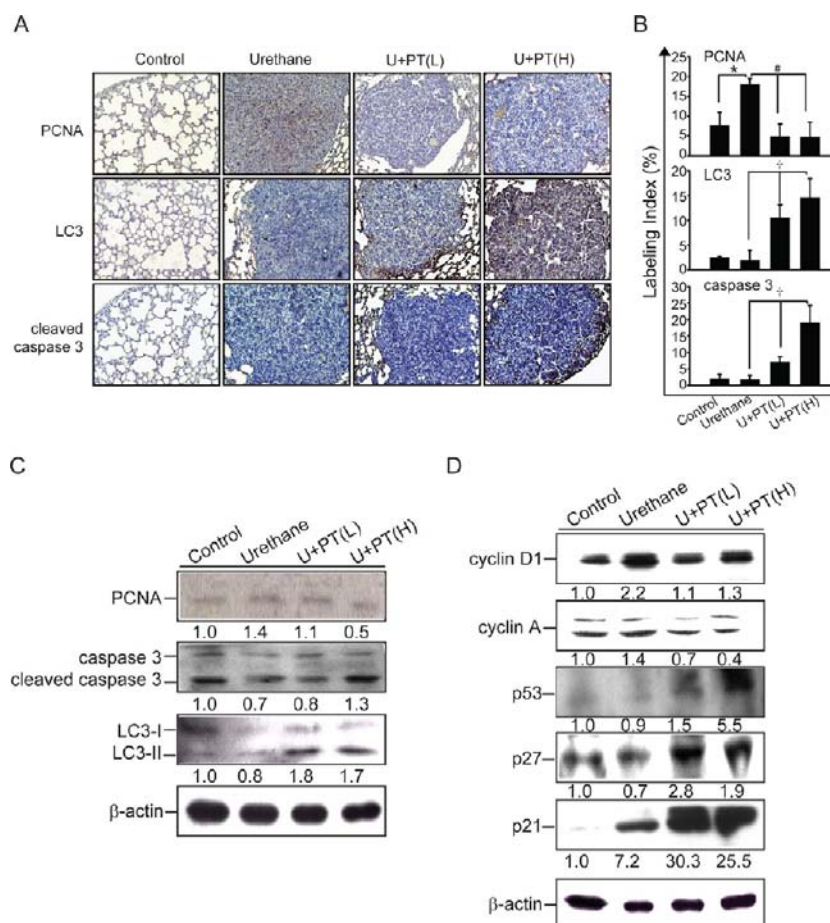


Figure 5. PT decreased cell proliferation and induced apoptosis and autophagy in neoplastic cells of urethane-exposed mice. (A) Immunohistochemistry (IHC) was used to detect the expression of PCNA (cell proliferation marker), cleaved caspase-3 (apoptosis marker), and LC3 (autophagy marker) in mouse lung tissues. (B) Quantitative IHC data represent the mean \pm SEM of three results in each group. *, $p < 0.05$, significantly higher than control group; #, $p < 0.05$, significantly lower than urethane-treated group; †, $p < 0.05$, significantly higher than urethane-treated group. (C) Expression of PCNA, cleaved caspase-3, and LC3 was confirmed by Western blotting of lung homogenates of A/J mice treated with the control, urethane, PT(L), and PT(H). (D) Analysis of proteins for cell cycle progression (cyclin D1, cyclin A), tumor suppressor p53, and CDK inhibitors (p21 and p27) in lung lysates of A/J mice treated with control (Con), urethane, PT(L), and PT(H). PT(L), pterostilbene low dose; 50 mg/kg; PT(H), pterostilbene high dose, 250 mg/kg. Each sample was run on separate Western blot, and the results of three independent experiments by using three individual mouse lungs were averaged. Representative data from one of three independent experiments are shown. Equal protein loading was determined by an anti- β -actin antibody. The number below each line indicates the relative intensity of protein expression compared to the control group (defined as 1).

study had been indicated that the plasma concentrations of pterostilbene at 30 min after ip administration (50 and 250 mg/kg) were estimated to be 2.24 and 26.85 $\mu\text{g/mL}$, respectively.²⁴ Previous study also indicated that following intravenous administration of pterostilbene, the glucuronidated pterostilbene can be detected in both serum and urine.⁸ As PT has limited aqueous solubility and limited oral bioavailability and there is little understanding of the metabolite of PT, these pose a barrier to its oral administration.²³ Hence, despite oral administration being a more meaningful route for a chemopreventive agent, to get precise understanding the mechanisms and the effects of PT in chemoprevention, mice were administered with PT by ip injection in our current study. Because the pharmacokinetics of PT was found to be more favorable than that of resveratrol and PT also has a relatively higher lipophilicity and better cell membrane permeability than those of resveratrol,²³ we suggest that it is still worthwhile to further investigate the chemopreventive and therapeutic effects of PT.

In the present study, A/J mice tolerated PT at doses of 50 and 250 mg/kg ip five times per week for 21 continuous weeks without weight loss or mortality, indicating that no measurable toxicity was seen in animals treated with PT. With regard to the effects of PT treatment, classification of lung surface tumors into different sizes showed that the lower multiplicity of tumors in mice given PT plus urethane was due to a substantial reduction in the number of larger tumors (Figures 2 and 3). Adenomas $>1.5 \text{ mm}^3$ were nearly completely inhibited by high-dose PT. The effect of PT on bigger tumors is potentially important because tumor size is a key determinant of the survival of lung cancer patients.²⁵ The results showed that surface lung tumor incidence was not altered by pterostilbene. This was not unexpected because the most sensitive indicator in the A/J mouse lung tumorigenesis model is tumor multiplicity. On the basis of the obvious effects on limiting lung tumor development and lack of detectable toxicities, we suggest that PT is a leading candidate to be evaluated for use in lung cancer chemoprevention.

It is reported that urethane metabolism occurs via two major pathways. The first pathway is catalyzed by esterase, leading to the formation of CO₂, NH₃, and ethanol.²⁶ This pathway is now recognized as a detoxification pathway and could not account for the potent genotoxicity and carcinogenicity of urethane. The second pathway is thought to involve oxidative metabolism via CYP enzymes and was thought as a bioactivation pathway. Previous study had proved that CYP2E1-mediated oxidation is the primary pathway responsible for 96% urethane bioactivation via epoxidation and subsequent genotoxicity and carcinogenicity.²⁷ Only about 3.5% urethane is metabolized by CYPs other than CYP2E1.²⁶ Following epoxidation, urethane is known to induce activation of K-Ras and deregulation of the p53 pathway. Once urethane-induced initiation occurs, sustained cellular proliferation will favor clonal expansion of the initiated cells and, combined with additional genetic damage, lead to tumor promotion and tumor progression.²⁷ Therefore, Ghanaym et al. reported a significant reduction of urethane-induced carcinogenicity in *CYP2e1*^{-/-} mice compared to *CYP2e1*^{+/+} mice and proved the essential role of CYP2E1-mediated oxidation in urethane-induced carcinogenicity. It has been reported that pterostilbene inhibits the activity of CYP1A1, CYP1A2, and CYP1B1 but not CYP2E1 in vitro.²⁸ As a result, pretreatment of pterostilbene 1 week prior to urethane administration in the current experiment may not alter the metabolism or activation of urethane directly. Interestingly, the mechanism of PT in lung cancer chemoprevention is not completely understood. We assessed the chemopreventive effects of PT using a model based on urethane-induced lung tumorigenesis, which is a suitable model for testing PT for lung cancer prevention because the molecular signatures are similar to lung human adenocarcinoma, including parallel changes in expression for glycolytic enzymes, cell cycle proteins, and genes related to angiogenesis.²⁹ Among these targets, EGFR and its downstream signaling pathways are important in the development of lung cancer. Therefore, understanding the effects of PT on EGFR and its downstream effectors could help to develop a novel chemopreventive strategy. Our experiments showed that the treatment of mice with PT leads to a decrease in the expression of EGFR and the downstream mediators, including Akt/mTOR, ERK1/2, Stat3, and NFκB, in urethane-induced lung tumors (Figure 4). Akt/mTOR is one of the most frequently hyperactivated signaling pathways in lung cancer. The knockdown of Akt activity is sufficient to suppress Akt-1 related signals important for protein translation and cell cycle progression, thus inhibiting lung cancer development.³⁰ The activation of Akt/mTOR also cooperated with other prosurvival pathways such as ERK1/2 and Stat3 to induce more progressive lung cancers.²⁰ Zhang et al. further indicated that the EGFR-PI3K-Akt-ERK signaling pathway could be a potential target of therapy directed toward the inflammatory microenvironment of lung cancer.

We also examined the effects of PT on the inhibition of Stat3 and NFκB transcription factors, which play major roles in inflammation and lung tumorigenesis. Stat3 and NFκB regulate transformation from normal cells to tumor cells, tumor cell survival, proliferation, invasion, angiogenesis, and metastasis.³¹ The suppression of Stat3 and NFκB pathways could also be an ideal strategy for the prevention and treatment of cancer.³² For example, resveratrol and its analogue were reported to inhibit both Stat3 and NFκB pathways in cancer cells, resulting in apoptosis and antiproliferation.³³ Ramasamy et al. also indicated that silibinin-mediated decreases in tumor number

and size correlate with the inhibition of cell proliferation and angiogenesis, most likely through the inhibition of iNOS expression involving down-regulation of Stat3 and NFκB signaling.³⁴ These studies indicated that Stat3 and NFκB are important targets for chemoprevention by natural products and strongly support our observation that suppression of Stat3 and NFκB by PT may counteract urethane-induced lung tumorigenesis (Figure 4).

Previous studies have indicated that Akt/mTOR, ERK1/2, Stat3, and NFκB can increase the expression of several factors in cell cycle progression, such as cyclins D and E. These pathways also play critical roles in carcinogenesis by blocking apoptosis through various mechanisms. Our current studies also indicate the complexity of molecular mechanisms in the regulation of cancer growth through cross-talk among EGFR, Akt/mTOR, ERK1/2, Stat3, NFκB, and even other signaling pathways in lung cancer. Thus, inhibition of these signaling pathways may contribute to cancer cell death by inducing cell cycle arrest, apoptosis, or autophagy. Indeed, our results demonstrated that PT suppressed the expression of proteins important for cell cycle regulation, such as cyclin D1, cyclin A, and PCNA (Figure 5). Cyclin D1 is required for cell cycle G1/S transition and is identified as a key downstream effector of EGFR in lung cancer. Our results are supported by the finding that EGFR downstream mediators (Akt/mTOR, ERK1/2, Stat3, and NFκB) are associated with cyclin D1 up-regulation, which disrupts the G1/S transition and leads to abnormal cell proliferation during urethane-induced lung carcinogenesis.

It has been reported that the expression of CDK inhibitors is reduced in lung cancer and is associated with tumor aggressiveness and poor prognosis.³⁵ The down-regulation of CDK inhibitors could be mediated by Ras, Akt, or MAPK activation or by increased Skp2 expression.³⁶ The inhibition of PI3K/Akt signaling resulted in higher levels of p21 and p27, leading to an attenuation of doxorubicin resistance in lung cancer cells. In addition to these signaling pathways, p21 can be up-regulated by p53 in lung cancer.³⁷ Consistent with these findings, we suggest that the aberrant expression of p21 and p27 in urethane-induced tumors is an active process regulated by the PI3K/Akt signaling pathway and that the restored expression of CDK inhibitors can be achieved by attenuating Akt activation and the induction of p53 expression after PT treatment (Figure 5). Studies in several tumor types indicated that the expression levels of CDK inhibitors have prognostic and therapeutic implications.^{38,39} Nevertheless, our results also showed that urethane induced p21 overexpression without apparent change of p53 (Figure 5C). It has been reported that expression of p21 could be regulated by p53-dependent or -independent mechanisms. The p53-independent transactivation of p21 is regulated by various proteins including Ras oncogene, transcriptional factors (such as SP1, SP3, MOX2, BETA2, HOXA10, STATs), and protein kinases.⁴⁰ Given that p21 has tumor suppressor activity, recent data suggest that it may behave as an oncogene in certain cellular contexts.⁴⁰ However, it is not clear whether p21 overexpression in the urethane-treated group contributes to lung tumorigenesis or an event in response to oxidative damage induced by urethane. Thus, it is worthwhile to further study the complicated molecular pathways regulating CDK inhibitors (such as p27 and p21) and to delineate the function of p21 induction in response to urethane or PT for designing a potential preventive and therapeutic strategy through induction of growth arrest in human cancers via PT treatment.

It has been reported that chemopreventive agents can target neoplastic cells to block cancer progression by inducing cell differentiation, modulating cell signaling, inhibiting the activity of oncogenes, inducing apoptosis and autophagy, and inhibiting metastasis.¹⁸ Accordingly, we investigated apoptosis and autophagy induced by PT treatment. Autophagy can minimize cellular damage in the response to acute stress, including hypoxia, oxidation, and heat shock, all of which contribute to protein dysfunction and genomic damage. Thus, autophagy limits the accumulation of cellular damage to proteins, organelles, and DNA, all of which can contribute to mutation, metabolic dysfunction, and initiate transformation.¹⁹ To this end, agonists of the autophagy pathway will most likely inhibit transformation and prevent cancer by limiting damage.¹⁹ Moving forward, the oncology field has considered taking a specific approach by targeting key components of the autophagy pathway to inhibit tumorigenesis. Although thousands of phytochemicals have been identified to date, few have been rigorously assessed for their ability to modulate autophagy. Herein, we found that PT induced significantly increased autophagy parallel to apoptosis compared to urethane-treated groups (Figure 5). Thus, PT could be a promising chemopreventive agent for lung tumorigenesis, mainly through its roles in cell cycle inhibition and activation of apoptosis and autophagy.

Cancer cell growth is driven by multiple signaling pathways and arises through a complex, multistep process by which cancer cells acquire the characteristics of unlimited proliferative potential and generate their own growth signals, thereby reducing dependence on exogenous growth stimulation and resistance to apoptosis and autophagy. Therefore, blocking only one specific pathway might not be sufficient to inhibit the growth of cancer cells. Chemopreventive agents such as phytochemicals, regulating multitargets, hold promise for improved chemopreventive effects that would be better than single-target inhibitors.⁴¹ In accordance with these studies, our current study emphasized the importance of PT for lung cancer prevention through in vivo research by modulating several targets important for lung tumorigenesis including EGFR, Akt/mTOR, Stat3, ERK1/2, and NF κ B pathways, leading to cell cycle arrest, the activation of apoptosis, and autophagy. Our results also indicated that pterostilbene has relatively low toxicity and that it can be used for a long period of time. Considering these beneficial effects, we strongly suggest that the multitargeting PT deserves further consideration for chemoprevention of lung cancer.

AUTHOR INFORMATION

Corresponding Author

* (C.-H.W.) Postal address: Department of Surgery, School of Medicine, Taipei Medical University—Shuang Ho Hospital, 291 Jhongheng Road, Jhonghe City, Taipei County 23561, Taiwan. Phone: 886-2-2249-0088, ext. 8810. Fax: 886-2-2248-0900. E-mail: chwu@tmu.edu.tw. (Y.-J.W.) Postal address: Department of Environmental and Occupational Health, National Cheng Kung University Medical College, 138 Sheng-Li Road, Tainan 70428, Taiwan. Phone: 886-6-235-3535, ext. 5804. Fax: 886-6-275-2484. E-mail: yjwang@mail.ncku.edu.tw.

Author Contributions

^{||}R.-J.C. and Y.-S.H. contributed equally to this work.

Funding

We thank the commission of this study by the National Science Council (NSC 100-2314-B-006-055), Food and Drug Administration, Department of Health, Executive Yuan (DOH101-FDA-41301), and Taipei Medical University, Center of Excellence for Cancer Research (TMU-CECR, DOH101-TD-C-111-008), for their support.

Notes

The authors declare no competing financial interest.

REFERENCES

- (1) Jemal, A.; Bray, F.; Center, M. M.; Ferlay, J.; Ward, E.; Forman, D. Global cancer statistics. *CA Cancer J. Clin.* **2011**, *61*, 69–90.
- (2) Vahakangas, K. TP53 mutations in workers exposed to occupational carcinogens. *Hum. Mutat.* **2003**, *21*, 240–251.
- (3) Keith, R. L. Chemoprevention of lung cancer. *Proc. Am. Thorac. Soc.* **2009**, *6*, 187–193.
- (4) Rimando, A. M.; Cuendet, M.; Desmarchelier, C.; Mehta, R. G.; Pezzuto, J. M.; Duke, S. O. Cancer chemopreventive and antioxidant activities of pterostilbene, a naturally occurring analogue of resveratrol. *J. Agric. Food Chem.* **2002**, *50*, 3453–3457.
- (5) McCormack, D.; McFadden, D. Pterostilbene and cancer: current review. *J. Surg. Res.* **2011**, *173*, e53–e61.
- (6) Chiou, Y. S.; Tsai, M. L.; Nagabhusanam, K.; Wang, Y. J.; Wu, C. H.; Ho, C. T.; Pan, M. H. Pterostilbene is more potent than resveratrol in preventing azoxymethane (AOM)-induced colon tumorigenesis via activation of the NF-E2-related factor 2 (Nrf2)-mediated antioxidant signaling pathway. *J. Agric. Food Chem.* **2011**, *59*, 2725–2733.
- (7) Ferrer, P.; Asensi, M.; Segarra, R.; Ortega, A.; Benlloch, M.; Obrador, E.; Varea, M. T.; Asensio, G.; Jorda, L.; Estrela, J. M. Association between pterostilbene and quercetin inhibits metastatic activity of B16 melanoma. *Neoplasia* **2005**, *7*, 37–47.
- (8) Remsberg, C. M.; Yanez, J. A.; Ohgami, Y.; Vega-Villa, K. R.; Rimando, A. M.; Davies, N. M. Pharmacometrics of pterostilbene: preclinical pharmacokinetics and metabolism, anticancer, antiinflammatory, antioxidant and analgesic activity. *Phytother. Res.* **2008**, *22*, 169–179.
- (9) Chen, R. J.; Ho, C. T.; Wang, Y. J. Pterostilbene induces autophagy and apoptosis in sensitive and chemoresistant human bladder cancer cells. *Mol. Nutr. Food Res.* **2010**, *54*, 1819–1832.
- (10) Suh, N.; Paul, S.; Hao, X.; Simi, B.; Xiao, H.; Rimando, A. M.; Reddy, B. S. Pterostilbene, an active constituent of blueberries, suppresses aberrant crypt foci formation in the azoxymethane-induced colon carcinogenesis model in rats. *Clin. Cancer Res.* **2007**, *13*, 350–355.
- (11) Paul, S.; DeCastro, A. J.; Lee, H. J.; Smolarek, A. K.; So, J. Y.; Simi, B.; Wang, C. X.; Zhou, R.; Rimando, A. M.; Suh, N. Dietary intake of pterostilbene, a constituent of blueberries, inhibits the β -catenin/p65 downstream signaling pathway and colon carcinogenesis in rats. *Carcinogenesis* **2010**, *31*, 1272–1278.
- (12) Chiou, Y. S.; Tsai, M. L.; Wang, Y. J.; Cheng, A. C.; Lai, W. M.; Badmaev, V.; Ho, C. T.; Pan, M. H. Pterostilbene inhibits colorectal aberrant crypt foci (ACF) and colon carcinogenesis via suppression of multiple signal transduction pathways in azoxymethane-treated mice. *J. Agric. Food Chem.* **2010**, *58*, 8833–8841.
- (13) Ikeda, K.; Nomori, H.; Ohba, Y.; Shibata, H.; Mori, T.; Honda, Y.; Iyama, K.; Kobayashi, T. Epidermal growth factor receptor mutations in multicentric lung adenocarcinomas and atypical adenomatous hyperplasias. *J. Thorac. Oncol.* **2008**, *3*, 467–471.
- (14) Janku, F.; Garrido-Laguna, I.; Petruzella, L. B.; Stewart, D. J.; Kurzrock, R. Novel therapeutic targets in non-small cell lung cancer. *J. Thorac. Oncol.* **2011**, *6*, 1601–1612.
- (15) Zhang, Z.; Stiegler, A. L.; Boggon, T. J.; Kobayashi, S.; Halmos, B. EGFR-mutated lung cancer: a paradigm of molecular oncology. *Oncotarget* **2010**, *1*, 497–514.

- (16) Uribe, P.; Gonzalez, S. Epidermal growth factor receptor (EGFR) and squamous cell carcinoma of the skin: molecular bases for EGFR-targeted therapy. *Pathol. Res. Pract.* **2011**, *207*, 337–342.
- (17) Tang, X.; Shigematsu, H.; Bekele, B. N.; Roth, J. A.; Minna, J. D.; Hong, W. K.; Gazdar, A. F.; Wistuba, I. I. EGFR tyrosine kinase domain mutations are detected in histologically normal respiratory epithelium in lung cancer patients. *Cancer Res.* **2005**, *65*, 7568–7572.
- (18) Malkinson, A. M. Primary lung tumors in mice as an aid for understanding, preventing, and treating human adenocarcinoma of the lung. *Lung Cancer* **2001**, *32*, 265–279.
- (19) Steeves, M. A.; Dorsey, F. C.; Cleveland, J. L. Targeting the autophagy pathway for cancer chemoprevention. *Curr. Opin. Cell Biol.* **2010**, *22*, 218–225.
- (20) Zhang, Y.; Wang, L.; Zhang, M.; Jin, M.; Bai, C.; Wang, X. Potential mechanism of interleukin-8 production from lung cancer cells: an involvement of EGF-EGFR-PI3K-Akt-Erk pathway. *J. Cell Physiol.* **2012**, *227*, 35–43.
- (21) Harhaj, E. W.; Dixit, V. M. Regulation of NF- κ B by deubiquitinases. *Immunol. Rev.* **2012**, *246*, 107–124.
- (22) Gullett, N. P.; Ruhul Amin, A. R.; Bayraktar, S.; Pezzuto, J. M.; Shin, D. M.; Khuri, F. R.; Aggarwal, B. B.; Surh, Y. J.; Kucuk, O. Cancer prevention with natural compounds. *Semin. Oncol.* **2010**, *37*, 258–281.
- (23) Lin, H. S.; Yue, B. D.; Ho, P. C. Determination of pterostilbene in rat plasma by a simple HPLC-UV method and its application in pre-clinical pharmacokinetic study. *Biomed. Chromatogr.* **2009**, *23*, 1308–1315.
- (24) Pan, M. H.; Chiou, Y. S.; Chen, W. J.; Wang, J. M.; Badmaev, V.; Ho, C. T. Pterostilbene inhibited tumor invasion via suppressing multiple signal transduction pathways in human hepatocellular carcinoma cells. *Carcinogenesis* **2009**, *30*, 1234–1242.
- (25) Birim, O.; Kappetein, A. P.; Takkenberg, J. J.; van Klaveren, R. J.; Bogers, A. J. Survival after pathological stage IA nonsmall cell lung cancer: tumor size matters. *Ann. Thorac. Surg.* **2005**, *79*, 1137–1141.
- (26) Hoffler, U.; El-Masri, H. A.; Ghanayem, B. I. Cytochrome P450 2E1 (CYP2E1) is the principal enzyme responsible for urethane metabolism: comparative studies using CYP2E1-null and wild-type mice. *J. Pharmacol. Exp. Ther.* **2003**, *305*, 557–564.
- (27) Ghanayem, B. I. Inhibition of urethane-induced carcinogenicity in *cyp2e1*^{-/-} in comparison to *cyp2e1*^{+/+} mice. *Toxicol. Sci.* **2007**, *95*, 331–339.
- (28) Mikstacka, R.; Przybylska, D.; Rimando, A. M.; Baer-Dubowska, W. Inhibition of human recombinant cytochromes P450 CYP1A1 and CYP1B1 by trans-resveratrol methyl ethers. *Mol. Nutr. Food Res.* **2007**, *51*, 517–524.
- (29) Stearman, R. S.; Dwyer-Nield, L.; Zerbe, L.; Blaine, S. A.; Chan, Z.; Bunn, P. A., Jr.; Johnson, G. L.; Hirsch, F. R.; Merrick, D. T.; Franklin, W. A.; Baron, A. E.; Keith, R. L.; Nemenoff, R. A.; Malkinson, A. M.; Geraci, M. W. Analysis of orthologous gene expression between human pulmonary adenocarcinoma and a carcinogen-induced murine model. *Am. J. Pathol.* **2005**, *167*, 1763–1775.
- (30) Xu, C. X.; Jere, D.; Jin, H.; Chang, S. H.; Chung, Y. S.; Shin, J. Y.; Kim, J. E.; Park, S. J.; Lee, Y. H.; Chae, C. H.; Lee, K. H.; Beck, G. R., Jr.; Cho, C. S.; Cho, M. H. Poly(ester amine)-mediated, aerosol-delivered Akt1 small interfering RNA suppresses lung tumorigenesis. *Am. J. Res. Crit. Care Med.* **2008**, *178*, 60–73.
- (31) Aggarwal, B. B.; Kunnumakkara, A. B.; Harikumar, K. B.; Gupta, S. R.; Tharakan, S. T.; Koca, C.; Dey, S.; Sung, B. Signal transducer and activator of transcription-3, inflammation, and cancer: how intimate is the relationship? *Ann. N.Y. Acad. Sci.* **2009**, *1171*, 59–76.
- (32) Luqman, S.; Pezzuto, J. M. NF κ B: a promising target for natural products in cancer chemoprevention. *Phytother. Res.* **2010**, *24*, 949–963.
- (33) Bhardwaj, A.; Sethi, G.; Vadhan-Raj, S.; Bueso-Ramos, C.; Takada, Y.; Gaur, U.; Nair, A. S.; Shishodia, S.; Aggarwal, B. B. Resveratrol inhibits proliferation, induces apoptosis, and overcomes chemoresistance through down-regulation of STAT3 and nuclear factor- κ B-regulated antiapoptotic and cell survival gene products in human multiple myeloma cells. *Blood* **2007**, *109*, 2293–2302.
- (34) Ramasamy, K.; Dwyer-Nield, L. D.; Serkova, N. J.; Hasebroock, K. M.; Tyagi, A.; Raina, K.; Singh, R. P.; Malkinson, A. M.; Aggarwal, R. Silibinin prevents lung tumorigenesis in wild-type but not in iNOS^{-/-} mice: potential of real-time micro-CT in lung cancer chemoprevention studies. *Clin. Cancer Res.* **2011**, *17*, 753–761.
- (35) Singhal, S.; Vachani, A.; Antin-Ozerkis, D.; Kaiser, L. R.; Albelda, S. M. Prognostic implications of cell cycle, apoptosis, and angiogenesis biomarkers in non-small cell lung cancer: a review. *Clin. Cancer Res.* **2005**, *11*, 3974–3986.
- (36) Kelly-Spratt, K. S.; Philipp-Staheli, J.; Gurley, K. E.; Hoon-Kim, K.; Knoblaugh, S.; Kemp, C. J. Inhibition of PI-3K restores nuclear p27Kip1 expression in a mouse model of Kras-driven lung cancer. *Oncogene* **2009**, *28*, 3652–3662.
- (37) Wang, Y.; James, M.; Wen, W.; Lu, Y.; Szabo, E.; Lubet, R. A.; You, M. Chemopreventive effects of pioglitazone on chemically induced lung carcinogenesis in mice. *Mol. Cancer Ther.* **2010**, *9*, 3074–3082.
- (38) Chu, I. M.; Hengst, L.; Slingerland, J. M. The Cdk inhibitor p27 in human cancer: prognostic potential and relevance to anticancer therapy. *Nat. Rev. Cancer* **2008**, *8*, 253–267.
- (39) Dworakowska, D.; Jassem, E.; Jassem, J.; Karmolinski, A.; Lapinski, M.; Tomaszewski, D.; Rzyman, W.; Jaskiewicz, K.; Sworcak, K.; Grossman, A. B. Prognostic value of the apoptotic index analysed jointly with selected cell cycle regulators and proliferation markers in non-small cell lung cancer. *Lung Cancer* **2009**, *66*, 127–133.
- (40) Abbas, T.; Dutta, A. p21 in cancer: intricate networks and multiple activities. *Nat. Rev. Cancer* **2009**, *9*, 400–414.
- (41) Mencher, S. K.; Wang, L. G. Promiscuous drugs compared to selective drugs (promiscuity can be a virtue). *BMC Clin. Pharmacol.* **2005**, *5*, 3.